

This is the accepted manuscript made available via CHORUS. The article has been published as:

Single-hole wave function in two dimensions: A case study of the doped Mott insulator

Shuai Chen, Qing-Rui Wang, Yang Qi, D. N. Sheng, and Zheng-Yu Weng

Phys. Rev. B **99**, 205128 — Published 17 May 2019

DOI: [10.1103/PhysRevB.99.205128](https://doi.org/10.1103/PhysRevB.99.205128)

Single-hole wave function in two dimensions: A case study of the doped Mott insulator

Shuai Chen,¹ Qing-Rui Wang,² Yang Qi,^{3,4,5} D. N. Sheng,⁶ and Zheng-Yu Weng^{1,7}

¹*Institute for Advanced Study, Tsinghua University, Beijing, 100084, China*

²*Department of Physics, The Chinese University of Hong Kong, Shatin, New Territories, Hong Kong, China*

³*Center for Field Theory and Particle Physics, Department of Physics, Fudan University, Shanghai 200433, China*

⁴*State Key Laboratory of Surface Physics, Fudan University, Shanghai 200433, China*

⁵*Collaborative Innovation Center of Advanced Microstructures, Nanjing 210093, China*

⁶*Department of Physics and Astronomy, California State University, Northridge, CA, 91330, USA*

⁷*Collaborative Innovation Center of Quantum Matter, Tsinghua University, Beijing, 100084, China*

(Dated: April 29, 2019)

We study a ground-state ansatz for the single-hole doped t - J model in two dimensions via a variational Monte Carlo (VMC) method. Such a single-hole wave function possesses finite angular momenta generated by hidden spin currents, which give rise to a novel ground state degeneracy in agreement with recent exact diagonalization (ED) and density matrix renormalization group (DMRG) results. We further show that the wave function can be decomposed into a quasiparticle component and an incoherent momentum distribution in excellent agreement with the DMRG results up to an 8×8 lattice. Such a two-component structure indicates the breakdown of Landau's one-to-one correspondence principle, and in particular, the quasiparticle spectral weight vanishes by a power law in the large sample-size limit. By contrast, turning off the phase string induced by the hole hopping in the so-called $\sigma \cdot t$ - J model, a conventional Bloch-wave wave function with a finite quasiparticle spectral weight can be recovered, also in agreement with the ED and DMRG results. The present study shows that a singular effect already takes place in the single-hole-doped Mott insulator, by which the bare hole is turned into a non-Landau quasiparticle with translational symmetry breaking. Generalizations to pairing and finite doping are briefly discussed.

CONTENTS

I. INTRODUCTION

I. Introduction	1	High-temperature superconductivity (HTS) in the cuprate ¹ is widely considered to be a strong correlation effect of the doped Mott insulator ² , where the pairing is not due to the phonon mechanism as in the original BCS theory ³ . In such a pure interacting electron system, the nature of the “normal state” prior to superconducting transition is crucial ^{2,4,5} in understanding the HTS mechanism.
II. The model and key results	3	In a conventional normal metal (Fermi liquid), each new particle injected into the system should behave like a Landau's quasiparticle at low energies. By contrast, in a non-Fermi-like Luttinger liquid ⁶ (LL), vanishing quasiparticle spectral weight has been identified in the one-dimensional (1D) doped Mott insulators, described by the Hubbard ⁷⁻⁹ and t - J model ^{10,11} . The generalization of a possible LL state to two dimensions (2D) in connection with the HTS cuprate has been conjectured ⁴ early on, but so far it has not been fully substantiated by either theory or experiment.
A. The t - J model	3	The key issue is how a doped hole propagates in the 2D quantum spin background of a doped Mott insulator as compared to a Fermi liquid. To this end, the study of a single-hole case has been of central interest as the simplest case of “normal state”. Considerable efforts have been invested in studying the single hole's motion in a 2D antiferromagnet described by the t - J model using both analytical and numerical techniques. Despite of a strong distortion induced by the hole in the spin background, which is generally known as the spin polaron effect, many early studies have concluded that the hole would still
B. Key results	3	
III. Ground state ansatz and variational Monte Carlo calculation	6	
A. Variational ground state for the one-hole doped Mott insulator	6	
B. Hidden spin/charge currents	7	
C. Nontrivial quantum number: Angular momentum $L_z = \pm 1$	8	
D. Equal-time single-hole propagation	9	
E. Momentum distribution $n^h(\mathbf{k})$ and quasiparticle spectral weight $Z_{\mathbf{k}}$	9	
F. The $\sigma \cdot t$ - J model: Bloch-wave-like ground state	10	
IV. Discussion	10	
V. Acknowledgements	11	
A. Variational ground state at half filling	12	
B. Variational Procedure	12	
References	13	

behave like a coherent quasiparticle with a finite spectral weight in the long-wavelength, low-energy regime. Shraiman and Siggia^{12,13} proposed a semiclassical variational wave function and an effective Hamiltonian which treats the twisted spin configuration as a dipolar distortion. In the self-consistent Born approximation^{14–18} (SCBA) approaches, spin magnon excitations renormalize the effective mass of a hole to result in a much reduced bandwidth as compared to the bare band parameters. The corresponding dispersion has the energy minima at momenta $\mathbf{K}^0 = (\pm\pi/2, \pm\pi/2)$, which agrees with the exact diagonalization (ED) finite-size calculations^{19,20}. Assuming a finite quasiparticle spectral weight and local minima at \mathbf{K}^0 , later efforts^{21–24} have been further devoted to issues like the detailed dispersion by including the next-nearest-neighbor hoppings, t' and t'' , in comparison with the angle-resolved photoemission spectroscopy (ARPES)^{25–28}.

However, a recent numerical study by ED and density matrix renormalization group (DMRG) has revealed²⁹ an important fact that, accompanying the single hole in the ground state, hidden spin currents are generically present in the background, which has been essentially overlooked in the previous numerical studies^{19,20} of the 2D t - J model. Namely, despite of a total momentum at $(\pm\pi/2, \pm\pi/2)$ under a periodic boundary condition (PBC), the doped hole itself may not always carry the full momentum since a part of it has been carried away by the spin current into the neutral spin background²⁹. Furthermore, under an open boundary condition (OBC) which maintains the lattice C_4 rotational symmetry, the ground state is characterized by finite angular momentum $L_z = \pm 1 \pmod{4}$, which is tied to the chiralities of the background spin currents with a double degeneracy²⁹. These are in sharp contrast to the above-mentioned spin polaron picture obtained by SCBA, which has suggested that the hole should be dressed by a *rigid* spin distortion at low energies that only renormalizes its effective mass, which still satisfies the Landau's one-to-one correspondence hypothesis such that the total momentum is fully carried by low-lying quasiparticle excitations.

Thus, the novel ground state degeneracy and associated spin currents found by numerical calculations²⁹ have clearly indicated that a single-hole ground state of the t - J model is not simply described by a conventional quasiparticle. Here one has to treat the local coupling between the hole and spin background more carefully as it may be much more singular than previously believed. This is critically important in order to meaningfully extrapolate the single-hole results into a large scale or a finite doping regime, where the local correlation dominated by the single hole's mutual influence with the spin background must be correctly taken into account as a proper starting point in order to understand pairing and other long-wavelength physics.

Therefore, in this work, we shall revisit the single-hole ground state of the 2D t - J model by studying a new ground state ansatz by variational Monte Carlo (VMC)

method. Such a variational state is the one-hole limit of the ground state ansatz previously constructed in the phase string theory^{30,31}. It has been already applied to the one-hole cases in the 1D^{11,32} as well as two-leg ladder³³ systems, with the VMC results well reproducing various singular features observed in the DMRG calculations. As opposed to the above-mentioned spin polaron^{12,13,15–18} or “spin bag” picture^{34,35}, a hole hopping on an antiferromagnetically correlated spin background will generally create a string-like spin mismatch defect, known as the phase string^{36–38}, which cannot be completely “self-healed” by the spin superexchange dynamics. In the SCBA scheme^{15–18}, the longitudinal S^z -string³⁹ induced by hopping is assumed to be reparable via the spin flip process of the Heisenberg term. However, the hopping of the hole will simultaneously generate the transverse S^x and S^y strings as well. An exact mathematical formulation^{36–38} has shown that after the S^z -string along the spin z -direction is “repaired” through spin flips, the transverse strings, represented by a sequence of *signs* known as the phase string, cannot be erased simultaneously and will be generally left in the hole path, which plays a role like the Berry phase to result in strong quantum interference once the whole paths of the hole are summed over in the Feynman's path-integral fashion. Namely, the doped holes will always create irreparable spin mismatch “strings” on its path to singularly influence its motion on a quantum spin background. Indeed, by precisely turning off such a phase string effect in the t - J model to result in the so-called σ - t - J model⁴¹, the above-outlined spin current pattern and novel ground state degeneracy all disappear to recover a true quasiparticle description as shown by ED and DMRG in Ref. 29.

Specifically, in this paper, we study such a single-hole variational ground state ansatz by VMC, in which the bare hole is “twisted” by producing a nonlocal phase shift due to the phase string effect based on the t - J model. It can correctly describe a one-hole quantum state with the conserved hole number $N_h = 1$, spin $S = S_z = 1/2$, and an angular momentum $L_z = \pm 1$ corresponding to a discrete C_4 rotation symmetry under the OBC. Namely, it has a novel double degeneracy for a given $S_z = 1/2$, corresponding to two chiralities of the neutral spin currents, all in agreement with the ED and DMRG results²⁹. Both the momentum distribution $n^h(\mathbf{k})$ and quasiparticle weight $Z_{\mathbf{k}}$ are in excellent agreement with the DMRG results up to an 8×8 lattice, showing that the hole wave function in the ground state can be decomposed into a quasiparticle component and an incoherent component with a broad continuous momentum distribution. In particular, $Z_{\mathbf{k}}$ is indeed peaked at four momenta $\mathbf{K}^0 = (\pm\pi/2, \pm\pi/2)$. But the finite-size scaling of $Z_{\mathbf{K}^0}$ shows a power-law decay, indicating the breakdown of the quasiparticle picture in the thermodynamic limit. The translational symmetry is explicitly broken in such a variational ground state. However, by turning off the phase string, all the above novel features disappear and the variational ground state recovers a simple Bloch-wave state in the σ - t - J model.

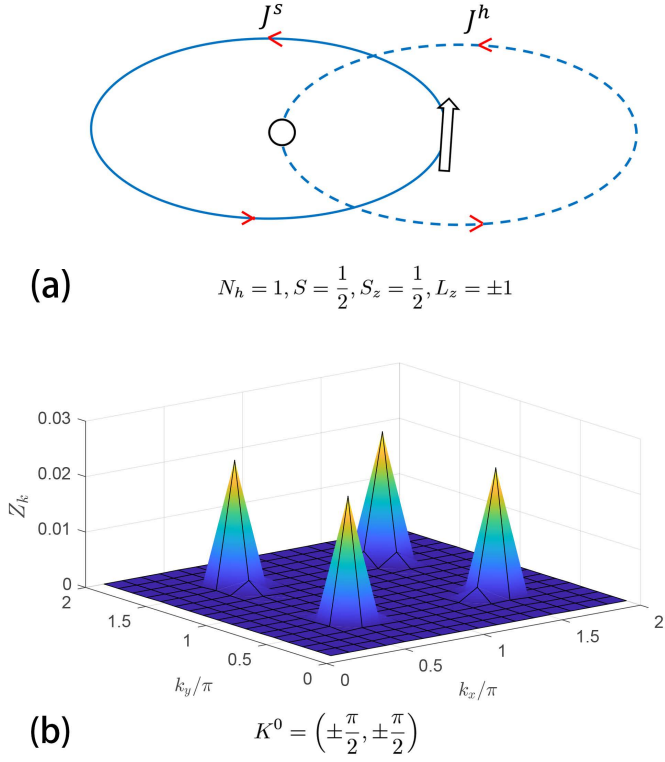


Fig. 1. (Color online.) (a) Schematic illustration of the single-hole wave function ansatz [Eq. (3)], in which the mutual entanglement between a hole and surrounding spins are explicitly characterized by the phase string operator [Eqs. (4) and (5)]. Such a single hole ground state can be labelled by the following quantum numbers: hole number $N_h = 1$, spin $S = 1/2$, $S_z = \pm 1/2$, and for a lattice with a discrete C_4 rotational symmetry, an angular momentum $L_z = \pm 1$ with nontrivial spin and hole currents, J_s and J_h , in agreement with the ED and DMRG results²⁹; (b) The quasiparticle spectral weight of the ground state (3) shows four sharp peaks at momenta $(\pm\pi/2, \pm\pi/2)$ at a finite size system ($N = 16 \times 16$).

Finally, a natural generalization of the present scheme to pairing and finite doping are briefly discussed in the end of the paper.

The rest of the paper is organized as follows. In Sec. II, we introduce the t - J model on a 2D square lattice and outline the key results. In Sec. III, we present the detailed composite structure of the single-hole variational ground state, which possesses the same quantum numbers as those identified in the previous ED and DMRG calculations. We further identify the two-component structure of the single-hole state of the t - J model. Two physical quantities, i.e., the momentum distribution $n^h(\mathbf{k})$ and quasiparticle spectral weight Z_k , are presented. For the $\sigma \cdot t$ - J model, a conventional Bloch-wave state is recovered. Finally, the summary and discussion along with some perspectives are given in Sec. IV.

II. THE MODEL AND KEY RESULTS

A. The t - J model

The model we consider in this work is the standard t - J model on a two-dimensional isotropic square lattice with the Hamiltonian $H_{t-J} = \mathcal{P} (H_t + H_J) \mathcal{P}$, in which

$$H_t = -t \sum_{\langle ij \rangle \sigma} c_{i\sigma}^\dagger c_{j\sigma} + \text{H.c.}, \quad (1)$$

$$H_J = J \sum_{\langle ij \rangle} \left(\mathbf{S}_i \cdot \mathbf{S}_j - \frac{1}{4} n_i n_j \right), \quad (2)$$

where the projective operator \mathcal{P} imposes the no-double-occupancy constraint on each site. Here, $c_{i\sigma}$ annihilates an electron at site i with spin σ , and $n_i = \sum_{\sigma} c_{i\sigma}^\dagger c_{i\sigma}$ and \mathbf{S}_i are the electron number and spin operator, respectively. We fix $t/J = 3$ in making comparison of the present VMC study of the variational ground state with the ED and DMRG results.

B. Key results

In this work, we study the following one-hole ground state ansatz for the 2D t - J model

$$|\Psi_G\rangle_{1h} = \sum_i \varphi_h(i) \tilde{c}_{i\downarrow} |\text{RVB}\rangle, \quad (3)$$

and show that it can systematically reproduce the numerical ED and DMRG results²⁹ via a VMC calculation. Here $|\text{RVB}\rangle$ denotes a *half-filled* spin background⁴², which is the ground state of the Heisenberg model H_J . The doped hole is created by the annihilation operator

$$\tilde{c}_{i\downarrow} = c_{i\downarrow} e^{-i\hat{\Omega}_i} \quad (4)$$

which removes an electron of spin \downarrow (without loss of generality) from the “vacuum” state $|\text{RVB}\rangle$, and at the same time, produces a nonlocal many-body “phase shift” $\hat{\Omega}_i$ in the spin background. The latter is defined by^{30,31}

$$\hat{\Omega}_i = \sum_l \theta_i(l) n_l^\downarrow, \quad (5)$$

in which in general $\theta_i(l)$ satisfies

$$\theta_i(l) = \theta_l(i) \pm \pi \quad (6)$$

and in particular, it takes the form $\theta_i(l) = \pm \text{Im} \ln(z_i - z_l)$ in 2D, with $z_i = x_i + iy_i$ as the complex coordinate of site i , and n_l^\downarrow denotes the number operator of \downarrow spin at site l . Finally, φ_h in Eq. (3) is a variational parameter representing the wave function of the doped hole, which is to be determined by minimizing the variational energy in the VMC calculation.

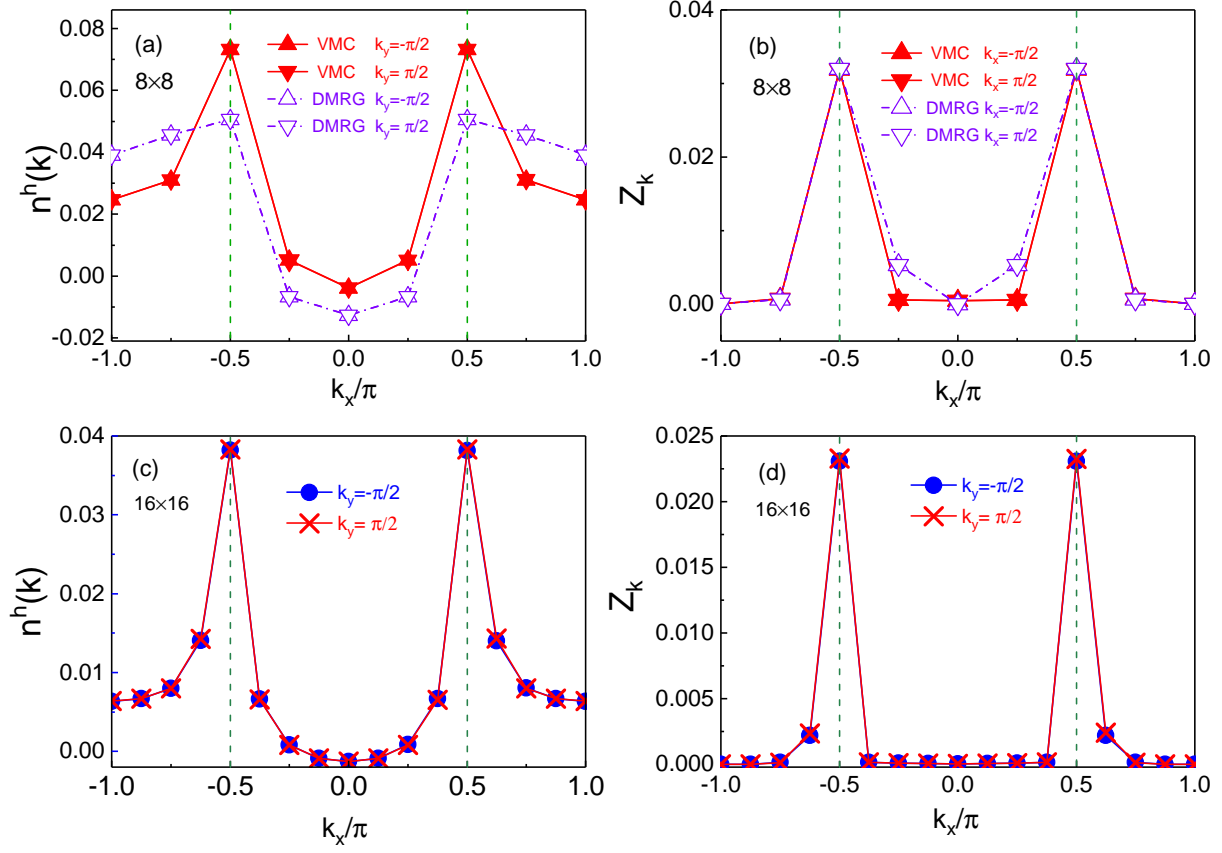


Fig. 2. (Color Online.) Momentum distribution of the hole, $n^h(\mathbf{k})$, and the quasiparticle weight $Z_{\mathbf{k}}$, as calculated by VMC in the ground state ansatz of Eq. (3): (a) and (b) show excellent agreement with the DMRG on a 8×8 lattice; (c) and (d): a larger size at 16×16 . The finite-size scaling results obtained by VMC are presented in Fig. 3.

Such a unique ansatz in Eq. (3) can be compared to the following Bloch-like one-hole state

$$|\Psi_{\text{Bloch}}\rangle_{1h} \propto \sum_i e^{i\mathbf{k}\cdot\mathbf{r}_i} c_{i\downarrow} |\text{RVB}\rangle. \quad (7)$$

Besides the momentum \mathbf{k} , the state of Eq. (7) carries a total spin $S = 1/2$, $S^z = 1/2$, and a charge $+e$, which is created by the bare hole operator $c_{i\downarrow}$ on a spin-singlet and translationally invariant spin background. So the new ground state of Eq. (3) means that the “quasiparticle” creation operator is changed to

$$c_{i\sigma} \rightarrow \tilde{c}_{i\sigma}, \quad (8)$$

or equivalently the single-hole wave function is changed from a Bloch wave to a many-body version by

$$e^{i\mathbf{k}\cdot\mathbf{r}_i} \rightarrow \varphi_h(i) e^{-i\hat{\Omega}_i}. \quad (9)$$

Indeed, the new quasiparticle, created by \tilde{c} in Eq. (3), can propagate more coherently as compared to the bare

c in the antiferromagnetic spin background (cf. Fig. 7). It is noted that the ansatz state in Eq. (3) is defined in a finite-size system with open boundary condition (OBC), in which the C_4 rotational symmetry is retained. Besides the total spin $S = 1/2$, $S^z = 1/2$, and the hole number $N_h = 1$, it shows a nontrivial angular momentum $L_z = \pm 1$ in agreement with the ED and DMRG²⁹, indicating that there is a novel double ground state degeneracy for a given S^z . Such a nontrivial angular momentum $L_z = \pm 1$ is shown to be associated with the neutral spin current pattern and charge current pattern, respectively, in Figs. 5 and 6. These currents are qualitatively consistent with the ED and DMRG results²⁹, which can be directly connected to the phase shift factor $e^{-i\hat{\Omega}_i}$ in the ground state of Eq. (3) as schematically illustrated in Fig. 1(a).

As shown in Fig. 1(b), the ground state of Eq. (3) is further composed of four Bloch-wave states [Eq. (7)] characterized by the quasiparticle spectral weight $Z_{\mathbf{k}}$, which

is peaked at four momenta

$$\mathbf{K}^0 = (\pm \frac{\pi}{2}, \pm \frac{\pi}{2}) . \quad (10)$$

$Z_{\mathbf{k}}$ measures the quasiparticle spectral weight, which shows that the ground state of Eq. (3) automatically includes four Bloch wave components at momenta \mathbf{K}^0 . This is consistent with the ED calculation where the four-fold degeneracy with the total momenta \mathbf{K}^0 has been identified on a torus (PBC) at a large ratio of t/J in the t - J model²⁹. In particular, the value of $Z_{\mathbf{k}}$ calculated by VMC agrees very well with that computed by DMRG for a lattice size $N = 8 \times 8$ under OBC as shown in Fig. 2(b) at $t/J = 3$.

Figure 2(d) further shows the VMC result of $Z_{\mathbf{k}}$ at $N = 16 \times 16$. In fact, at larger sample sizes, $Z_{\mathbf{k}}$ is shown to vanish in a power-law fashion (cf. Fig. 3(b)) as follows:

$$Z_{\mathbf{K}^0} \simeq 0.59 \frac{1}{L^{1.31}} \quad (11)$$

at $t/J = 3$ with L denoting the sample length. In other words, the ground state ansatz (3) is a prototypic non-Fermi liquid state with vanishing $Z_{\mathbf{k}}$ at $N \equiv L^2 \rightarrow \infty$. Such a “twisted” quasiparticle is non-Landau-like, in contrast to the conventional Landau quasiparticle implied in the Bloch-wave state (7).

Furthermore, the momentum structure of the doped hole can be also measured by the hole momentum distribution function defined by

$$n^h(\mathbf{k}) \equiv 1 - n^e(\mathbf{k}) = 1 - \left\langle \sum_{\sigma} c_{\mathbf{k}\sigma}^{\dagger} c_{\mathbf{k}\sigma} \right\rangle , \quad (12)$$

where $n^h(\mathbf{k}) = 0$ at half-filling and $\sum_{\mathbf{k}} n^h(\mathbf{k}) = 1$ for the one hole case. The good agreement between the VMC calculation based on Eq. (3) and the DMRG result at $N = 8 \times 8$ can be found in Fig. 2(a). Figure 2(c) further shows the VMC result at $N = 16 \times 16$. A finite-size scaling is presented in Fig. 3(a), which indicates that besides the peaks at \mathbf{K}^0 proportional to $Z_{\mathbf{K}^0}$, $n^h(\mathbf{k})$ exhibits a broad continuum, which satisfies a scaling $\propto 1/N$ and thus its total weight contributes to a finite and predominant part to the sum rule of $\sum_{\mathbf{k}} n^h(\mathbf{k})$. By contrast, the quasiparticle component vanishes as given in Eq. (11), such that the bare hole truly becomes incoherent in the thermodynamic limit demonstrated by extrapolation of finite size results.

Therefore, the one-hole ground state (3) is composed of two components, in which the doped hole either behaves like a Bloch wave at the four Fermi points of \mathbf{K}^0 with the spectral weight $Z_{\mathbf{K}^0}$ or becomes incoherent with a broad momentum distribution. In the later component, a partial momentum is carried away by the *neutral* spin currents as presented in Fig. 5. The Landau’s one-to-one correspondence hypothesis no longer holds true here in the presence of the second component, which violates the adiabaticity by allowing a continuous momentum transfer between the hole and the surrounding spin

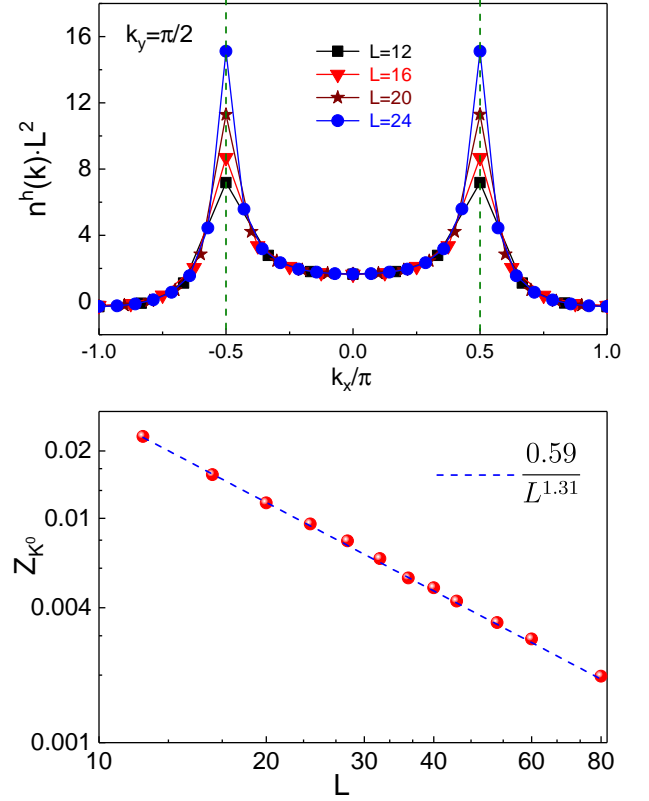


Fig. 3. (Color online.) The scaling analysis of the momentum distribution $n^h(\mathbf{k})$ and the quasiparticle weight $Z_{\mathbf{K}^0}$. (a) The broad background part of $n^h(\mathbf{k})$ scales with the inverse of L^2 in the square sample $N = L \times L$; (b) The quasiparticle weight $Z_{\mathbf{K}^0}$ at the peak momentum $\mathbf{K}^0 = (\pm \frac{\pi}{2}, \pm \frac{\pi}{2})$ vanishes in a power-law fashion by $L^{-1.31}$.

background. In particular, φ_h determined by VMC is no longer Bloch-wave-like (cf. Fig. 4(b)), which means the translational symmetry is explicitly broken.

Finally, we find that the Bloch-like ground state in Eq. (7) will replace Eq. (3) to become the ground state variationally for the $\sigma \cdot t$ - J model. All the novel properties including the double ground state degeneracy, non-trivial L^z with finite spin/charge currents surrounding the hole/spin, vanishing $Z_{\mathbf{k}}$, and the two-component feature, etc., disappear in such a ground state. In other words, we find that the Landau’s quasiparticle description for the doped hole is recovered in the model in which the phase string effect is turned off in the hopping term, while the superexchange term remains unchanged. Thus the present variational approach clearly establishes that the phase string effect hidden in the 2D t - J model is well encoded by the phase string operator in Eq. (5), which

gives rise to the mutual spin/charge currents as the composite structure associated with the doped hole that is “twisted” according to Eq. (4) in an antiferromagnetic background [RVB].

III. GROUND STATE ANSATZ AND VARIATIONAL MONTE CARLO CALCULATION

A. Variational ground state for the one-hole doped Mott insulator

The single-hole-doped ground state may be generally constructed by removing an electron with, say, \downarrow spin, from the half-filling ground state [RVB] as follows

$$|\Psi_G\rangle_{1h} = \sum_i \left(\varphi_h(i) \hat{\Pi}_i \right) c_{i\downarrow} |\text{RVB}\rangle, \quad (13)$$

where the summation is over the lattice site i weighted by a hole wave function $\varphi_h(i)$ and a many-body operator $\hat{\Pi}_i$, which denotes the generic distortion (i.e., spin polaron) of the spin background in response to the injection of a hole into the half-filling ground state.

The ground state of the Heisenberg type Hamiltonian H_J at half-filling is denoted by [RVB] above. So far the best variational wave function is the so-called *bosonic* resonant valence bond (RVB) state proposed⁴² by Liang, Doucot, and Anderson, which is a spin singlet with translational invariance, and has a very accurate variational energy $[E_G^0/(2N) + 1/4J = -0.3344J]$ as compared to the precise numerical results. Our VMC approach will be based on such an [RVB] as the starting point (Appendix A).

If one neglects the “spin polaron” effect of $\hat{\Pi}_i$ in Eq. (13) by taking $\hat{\Pi}_i = 1$, a Bloch-like state $|\Psi_{\text{Bloch}}\rangle_{1h}$ will be reproduced with

$$\varphi_h(i) \propto e^{i\mathbf{k}\cdot\mathbf{r}_i}, \quad (14)$$

as given in Eq. (7), which describes a Landau’s quasiparticle with the quantum numbers of total spin $S = 1/2$, $S^z = 1/2$, charge $+e$, and a momentum \mathbf{k} corresponding to the translational operation by a distance \mathbf{l} ,

$$\hat{T}_1 |\Psi_{\text{Bloch}}\rangle_{1h} = e^{-i\mathbf{k}\cdot\mathbf{l}} |\Psi_{\text{Bloch}}\rangle_{1h}, \quad (15)$$

by noting $\hat{T}_1 |\text{RVB}\rangle = |\text{RVB}\rangle$, $\hat{T}_1 c_{i\downarrow} \hat{T}_1^\dagger = c_{i+\mathbf{l}\downarrow}$.

Such a Bloch wave picture, marked by Eq. (14), would remain unchanged at $\hat{\Pi}_i \neq 1$ if one requires the translational symmetry (15) under a many-body operator \hat{T}_1 involving the hole and *whole* spins. (Note that $\hat{\Pi}_i$ generally satisfies the translational symmetry by $\hat{T}_1 \hat{\Pi}_i c_{i\downarrow} \hat{T}_1^\dagger = \hat{\Pi}_{i+\mathbf{l}} c_{i+\mathbf{l}\downarrow}$.) However, in the present variational scheme, $\varphi_h(i)$ obtained by VMC with $\hat{\Pi}_i \neq 1$ may not necessarily recover the Bloch-wave solution of Eq. (14). In other words, a spontaneous translational symmetry breaking may occur in the single-hole ground state (13), as to be shown below.

First, we note that the Bloch-wave state indeed holds true generally if $\hat{\Pi}_i$ represents a *local* spin distortion rigidly bound to the hole, solely specified by the hole or a “centre-of-mass” coordinate via the hole wave function $\varphi_h(i)$. Indeed, the “longitudinal spin polaron”^{15–18} or “spin bag” effect^{34,35} can generally improve the ground state energy of the Bloch state (7) without changing its nature as a Landau’s quasiparticle, except for a renormalization of the effective mass or even the location of \mathbf{k} in the ground state.

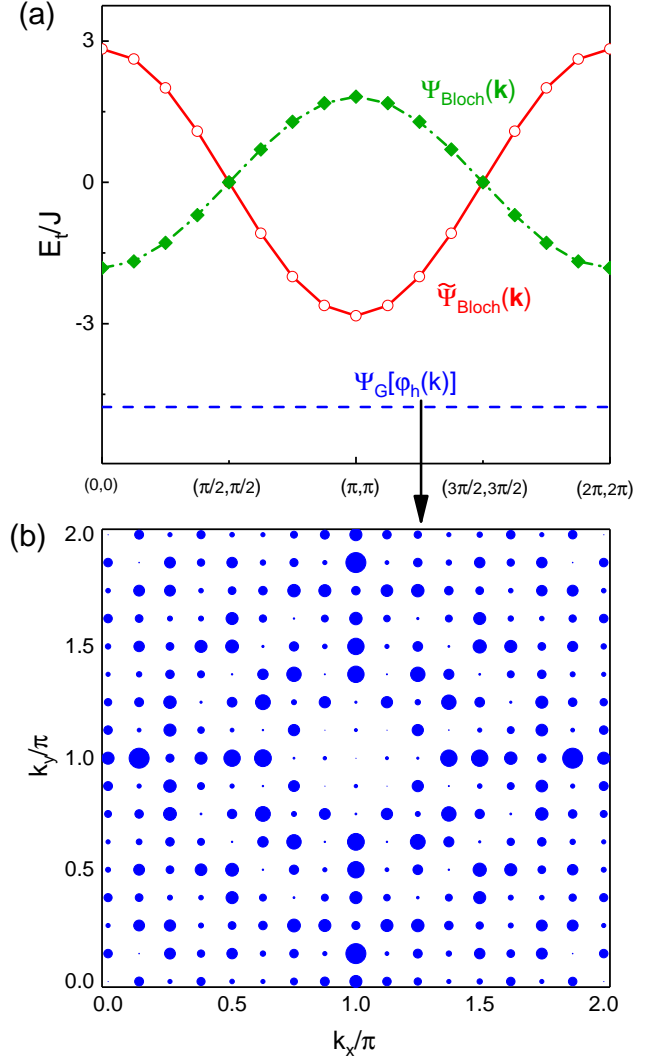


Fig. 4. (Color Online.) (a) The kinetic energies of the Bloch-like states $|\Psi_{\text{Bloch}}(\mathbf{k})\rangle_{1h}$ [Eq. (7)] and $|\tilde{\Psi}_{\text{Bloch}}(\mathbf{k})\rangle_{1h}$ [Eq. (17)] as a function of momentum vs. that of the variational ground state $|\Psi_G\rangle_{1h}$ in Eq. (3) (dashed line); Note that the hole wave function $\varphi_h(i)$ determined variationally in Eq. (3) is not translational invariant as shown in (b); (b) The distribution of the absolute value of $\varphi_h(\mathbf{k})$ as the Fourier transformation of $\varphi_h(i)$ in the momentum space.

However, in this work, we shall focus on a new type of

“transverse spin polaron” effect in $\hat{\Pi}_i$ given by^{30,31}

$$\hat{\Pi}_i = e^{-i\hat{\Omega}_i}, \quad (16)$$

where the many-body phase shift operator $\hat{\Omega}_i$ is defined in Eq. (5), which will introduce *transverse spin currents* around the hole (see below). The precise form of Eq. (5) is originated from the intrinsic phase string sign structures^{36–38} of the t - J model, representing a long-range mutual entanglement between the doped hole and the spin background. Physically, the phase shift in Eq. (16) describes a nonlocal response of the *whole* spin degree of freedom to the injection of a hole, which is non-perturbative in nature. Its explicit expressions in one-dimension^{11,32} and two-leg ladder^{33,43} systems have been previously studied in earlier works.

The VMC simulation (cf. Appendix B) shows that the ground state energy of the ansatz state (3) will be lowered as compared to that of the Bloch state (7) by $\Delta E_G = -1.50J$ at $N = 16 \times 16$ (in which the kinetic energy difference is $\Delta E_t = -2.71J$ and the superexchange energy difference is $\Delta E_J = 1.21J$). Here, the absolute value of $\varphi_h(\mathbf{k})$, the Fourier transformation of $\varphi_h(i)$ determined by optimizing the ground state energy, is shown in Fig. 4(b). Clearly it is not solely peaked at four \mathbf{K}^0 in Eq. (10) as would be expected for a linear superposition of four translational invariant states with total momenta \mathbf{K}^0 , which are to be obtained later by calculating the quasiparticle spectral weight.

In particular, if one assumes a translationally invariant form with $\varphi_h(i)$ taking the Bloch-wave form in Eq. (14)

$$|\tilde{\Psi}_{\text{Bloch}}(\mathbf{k})\rangle_{1h} \propto \sum_i e^{i\mathbf{k}\cdot\mathbf{r}_i} \tilde{c}_{i\downarrow} |\text{RVB}\rangle, \quad (17)$$

the resulting kinetic energy is *higher* by $\Delta E_t = 1.94J$ at $N = 16 \times 16$ (the superexchange energy is the same). Therefore, in contrast to Eq. (17), the wave function $\varphi_h(i)$ as determined variationally in Eq. (3) indeed automatically breaks the translational symmetry in the true variational ground state.

It is noted that the VMC calculation for an 8×8 square lattice with OBC ($t = 3J$) gives rise to a kinetic energy $E_t = -5.08J$ and the superexchange energy $E_J = -37.21J$ (at half-filling $E_J = -39.4884J$), while the DMRG gives the values of $E_t = -8.67J$ and $E_J = -37.28J$. Here we emphasize that one may further improve the single holes kinetic energy by incorporating the SCBA-like correction into the ansatz state (3) without changing the nature of the composite/fractionalization structure of the one-hole ground state. But the absolute kinetic energy is not our main concern here. Instead, we shall focus more on the structure and ground state properties of the ansatz state (3) in comparison with the DMRG simulation.

On the other hand, as we shall see later, with the phase string being switched off in the so-called $\sigma \cdot t$ - J model by restoring the trivial sign structure (cf. Sec. III F), the one-hole wave function will simply reduce to the Bloch

wave form in Eq. (7) with a lower ground state energy than that of Eq. (3). Thus, the phase shift operator of Eq. (5) is really originated from the phase string, which must be “turned off” in Eq. (13) in the absence of such an effect. Consequently $\varphi_h(i)$ restores the Bloch wave form in Eq. (14).

Although one may further improve the one-hole ground state energy by incorporating the “longitudinal spin polaron” effect^{12,13,15–18} mentioned above for both t - J and $\sigma \cdot t$ - J models, in the present work, our main focuses will be on the qualitatively different properties exhibited between the ground state of Eq. (3) and the Bloch-wave state in Eq. (7), and the conventional “longitudinal spin polaron” effect will be omitted for the sake of simplicity.

B. Hidden spin/charge currents

It can be explicitly seen that the ground state ansatz $|\Psi_G\rangle_{1h}$ in Eq. (3) has the hole number $N_h = 1$ and total spin $S = S^z = 1/2$, which are conserved in the t - J Hamiltonian. In the Heisenberg picture, the corresponding continuity equations associated with these quantities are given as follows²⁹

$$\frac{dn_i^h}{d\tau} = \sum_{j=\text{NN}(i)} J_{ij}^h, \quad (18)$$

$$\frac{dS_i^z}{d\tau} = \sum_{j=\text{NN}(i)} (J_{ij}^s + J_{ij}^b), \quad (19)$$

where τ denotes the time, J^h the hole (charge) current, J^b the backflow spin current associated with the hole hopping, and J^s the neutral spin current in the Heisenberg background, which are respectively defined by

$$J_{ij}^h = -it \sum_{\sigma} \left(c_{i\sigma}^\dagger c_{j\sigma} - c_{j\sigma}^\dagger c_{i\sigma} \right), \quad (20)$$

$$J_{ij}^b = i \frac{t}{2} \sum_{\sigma} \sigma \left(c_{i\sigma}^\dagger c_{j\sigma} - c_{j\sigma}^\dagger c_{i\sigma} \right), \quad (21)$$

$$J_{ij}^s = -\frac{J}{2} i (S_i^+ S_j^- - S_i^- S_j^+). \quad (22)$$

By using VMC, one can variationally determine the single hole wave function $\varphi_h(i)$ of the ansatz state (3). The corresponding instant patterns of spin currents around the hole and the hole currents around an \uparrow spin are obtained by computing the following correlation functions: $\langle \mathcal{P}_l^h J_{ij}^s \rangle$ and $\langle \mathcal{P}_m^s J_{ij}^h \rangle$ where $\mathcal{P}_l^h \equiv n_{i_0}^h$ and $\mathcal{P}_l^s \equiv c_{l\uparrow}^\dagger c_{l\uparrow}$ project the hole and an \uparrow spin at site l , as shown in Figs. 5 and 6, respectively. In Fig. 5, circulating neutral spin currents surrounding the doped hole are clearly shown, and mutually hole currents circulating a fixed (\uparrow) spin are presented in Fig. 6. Their chirality depends on the sign of $\hat{\Omega}_i$ in Eq. (5), which is concomitant with a double degeneracy of the ground state specified by an angular momentum $L_z = \pm 1$ to be discussed later.

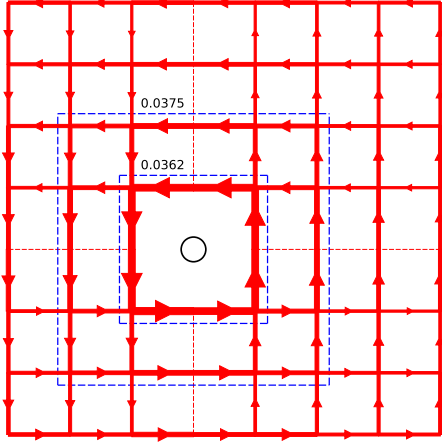


Fig. 5. (Color Online.) The neutral spin current (J_{ij}^s) pattern surrounding the hole in one of the degenerate ground states with $L_z = 1$ in a lattice of $N = 8 \times 8$ with OBC. (The red vertical and horizontal dashed lines mark the bonds with vanishing spin currents.) The dashed blue closed loops and numbers indicate the Wilson loops which count the Berry phase defined in Eq. (23).

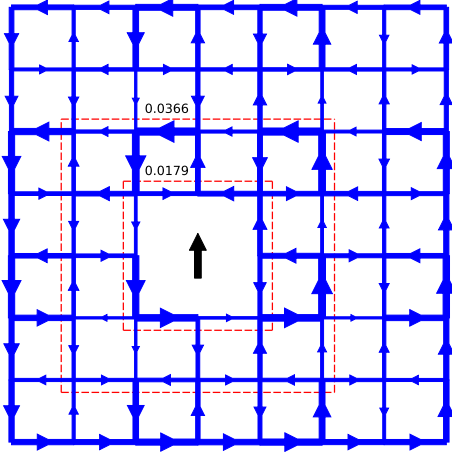


Fig. 6. (Color Online.) The charge (hole) current (J_{ij}^h) pattern surrounding an \uparrow spin projected onto a given lattice site in a degenerate ground state with $L_z = 1$ in a lattice of $N = 8 \times 8$ with OBC. The dashed red closed loops and numbers indicate the Wilson loops counting the Berry phase defined in Eq. (24).

These novel spin and charge currents can be directly traced back to the phase shift operator in Eq. (16), which can be associated with a nontrivial Berry phase⁴⁴. Generally, the Berry phase of Eq. (3) can be identified by its phase change accumulated under an adiabatic change of the wave function along a closed loop in some parameter space. Here it is specified by the space-time path of the hole and spin configurations.

If we examine a loop in the parameter space describing

the full braiding between such a spin and the doped hole, one would find two Berry phases, one corresponding to the winding of the spin at m around the hole at i_0 via a closed loop c encircling but not crossing i_0

$$\gamma_{i_0}^{h-s}[c] \propto W[c] \equiv \left\langle \oint_c \mathcal{P}_{i_0}^h J_{ij}^s \right\rangle, \quad (23)$$

and the other the winding of the hole around the spin, given by

$$\gamma_m^{s-h}[c] \propto T[c] \equiv \left\langle \oint_c \mathcal{P}_m^s J_{ij}^h \right\rangle. \quad (24)$$

Both nontrivial $\gamma_{i_0}^{h-s}[c]$ and $\gamma_m^{s-h}[c]$ are thus directly connected with the spin and charge current loops shown in Figs. 5 and 6.

C. Nontrivial quantum number: Angular momentum $L_z = \pm 1$

Let us start with a system of the square lattice of a finite size of $2M \times 2M$, which possesses a C_4 rotational symmetry under the OBC. A straightforward manipulation based on the wave function in Eq. (3) can demonstrate (see below) that under a spatial rotation of $\pi/2$, the ground state will be transformed by

$$\hat{R}(\pi/2)|\Psi_G\rangle_{1h} = \pm i|\Psi_G\rangle_{1h}, \quad (25)$$

where $\hat{R}(\theta)$ is the spatial rotational operator of angle θ with eigenvalue $e^{iL_z\theta}$. So the ground state has a nonzero angular momentum $L_z = \pm 1$ and a precise two-fold degeneracy under a given S^z , which are in agreement with the numerical result²⁹ for finite-size systems with $t/J = 3$.

The proof of Eq. (25) is given as followed. Let $\hat{R} \equiv \hat{R}(\pi/2)$ be the operator that rotates the system anticlockwisely by 90 degrees. When acting \hat{R} on the variational wave function (3), one has

$$\begin{aligned} \hat{R}|\Psi_G\rangle_{1h} &= \hat{R} \sum_i \varphi_h(i) e^{-i\hat{\Omega}_i} c_{i\downarrow} |\text{RVB}\rangle \\ &= \sum_i \varphi_h(i) \left(\hat{R} e^{-i\hat{\Omega}_i} c_{i\downarrow} \hat{R}^{-1} \right) \hat{R} |\text{RVB}\rangle. \end{aligned} \quad (26)$$

The spin RVB state by construction is rotationally invariant

$$\hat{R}|\text{RVB}\rangle = |\text{RVB}\rangle. \quad (27)$$

The symmetry transformation of the combination of the phase string operator and the fermion annihilation operator is

$$\begin{aligned} \hat{R} e^{-i\hat{\Omega}_i} c_{i\downarrow} \hat{R}^{-1} &= \hat{R} \exp \left(\pm i \sum_{l \neq i} \theta_l(l) n_{l\downarrow} \right) c_{i\downarrow} \hat{R}^{-1} \\ &= \exp \left(\pm i \sum_{l \neq i} \theta_l(l) n_{\hat{R}l\downarrow} \right) c_{\hat{R}i\downarrow}, \end{aligned}$$

which can be further simplified by using $\theta_{\hat{R}i}(\hat{R}l) = \theta_i(l) + \pi/2$ and $\sum_{l(\neq i)} n_{l\downarrow} = \sum_{l(\neq i)} \left(\frac{n_{l\downarrow} + n_{l\uparrow}}{2} - \frac{n_{l\uparrow} - n_{l\downarrow}}{2} \right) = \frac{N-1}{2} - S^z$. Therefore, the symmetry transformation of the wave function Eq. (26) becomes

$$\begin{aligned} & \hat{R}|\Psi_G\rangle_{1h} \\ &= \sum_i \varphi_h(i) \exp \left[\pm i \frac{\pi}{2} \left(\frac{N-1}{2} - S^z \right) \right] e^{-i\hat{\Omega}_i c_{i\downarrow}} |\text{RVB}\rangle \\ &= \exp \left[\pm i \frac{\pi}{2} \left(\frac{N-1}{2} - S^z \right) \right] |\Psi_G\rangle_{1h}. \end{aligned} \quad (28)$$

For a bipartite lattice with size $N = 2M \times 2M$ and $S^z = 1/2$, one finds that Eq. (25) holds true. On the other hand, for a lattice with odd number of total sites, for example, $N = 5 \times 5$, the phase factor in Eq. (28) is ± 1 . All these are consistent with ED and DMRG simulations²⁹.

D. Equal-time single-hole propagation

In the single-hole ground state, one may examine the single-hole propagator defined by

$$\mathcal{C}_{ij} = \langle \Psi_G | c_{j\downarrow} c_{i\downarrow}^\dagger | \Psi_G \rangle_{1h}. \quad (29)$$

The result calculated by VMC is presented in Fig. 7. We can see that the propagator \mathcal{C}_{ij} is substantially suppressed and decays much faster than in a conventional Bloch wave state of Eq. (7) (with the momentum at \mathbf{K}^0 for the convenience of comparison) as shown by \mathcal{C}_{ij}^0 in Fig. 7, which is defined by

$$\mathcal{C}_{ij}^0 = \langle \Psi_{\text{Bloch}} | c_{j\downarrow} c_{i\downarrow}^\dagger | \Psi_{\text{Bloch}} \rangle_{1h}. \quad (30)$$

It implies that the ground-state ansatz in Eq. (3) does not favor a coherent propagator of a bare hole on the quantum spin background.

We have seen that in the ground state ansatz (3), the doped hole is “twisted” into a composite hole described by $\tilde{c}_{i\downarrow}$ in Eq. (4). Thus, a new hole object characterized by $\tilde{c}_{i\downarrow}$ is expected to propagate more coherently in the following propagator:

$$\begin{aligned} \mathcal{D}_{ij} &= \langle \Psi_G | \tilde{c}_{j\downarrow} \tilde{c}_{i\downarrow}^\dagger | \Psi_G \rangle_{1h} \\ &= \varphi_h^*(j) \varphi_h(i) \left\langle \left(\frac{1}{2} - S_j^z \right) \left(\frac{1}{2} - S_i^z \right) \right\rangle_{\text{RVB}}, \end{aligned} \quad (31)$$

whose propagation over the spatial distance calculated by VMC is indeed much improved and in fact becomes comparable to the coherent Bloch-wave state characterized by \mathcal{C}_{ij}^0 as shown in Fig. 7. However, as indicated in Fig. 4(b), the hole wave function $\varphi_h(i)$ is no longer a Bloch wave and \mathcal{D}_{ij} must deviate from \mathcal{C}_{ij}^0 in the long-distance as to be shown below.

Thus, a bare hole created by $c_{i\downarrow}$ on the half-filling vacuum is no longer a stable elementary excitation to form

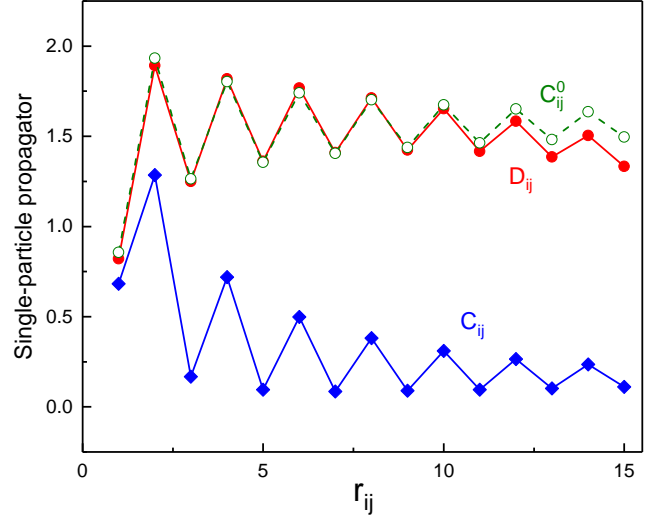


Fig. 7. (Color online.) The propagation amplitude of a bare hole, \mathcal{C}_{ij} , is much reduced as compared to that of the “twisted” hole, \mathcal{D}_{ij} , in the ground state ansatz (3). The latter is comparable to the hole propagation \mathcal{C}_{ij}^0 for a Bloch wave state defined in Eq. (7) (with momentum \mathbf{K}^0). Here the spatial distance $r_{ij} = |x_i - x_j| + |y_i - y_j|$, and \mathcal{C}_{ij} and \mathcal{D}_{ij} are calculated by averaging over all the lattice sites with each given distance r_{ij} based on the definitions given in Eq. (29) and Eq. (31), respectively. The lattice size is 20×20 .

a conventional Bloch wave. Instead, in the ground state, the doped hole will break down or fractionalize to become a new *composite* object, $\tilde{c}_{i\downarrow}$, which is composed of mutual spin and charge current patterns previously shown in Figs. 5 and 6, respectively. The residual bare hole component has a much reduced propagation amplitude as indicated in Fig. 7. In the following, we shall further look into the momentum structure of such a single-hole propagator in order to follow its long-distance behavior.

E. Momentum distribution $n^h(\mathbf{k})$ and quasiparticle spectral weight $Z_{\mathbf{k}}$

There are two basic physical quantities which can characterize the fate of the bare hole injected into the half-filling ground state. One is the Landau quasiparticle spectral weight $Z_{\mathbf{k}}$ defined by⁴⁵

$$\begin{aligned} Z_{\mathbf{k}} &\equiv \left| \langle \text{RVB} | c_{\mathbf{k}\downarrow}^\dagger | \Psi_G \rangle_{1h} \right|^2 \\ &= \frac{1}{2} \left| \langle \Psi_{\text{Bloch}}(\mathbf{k}) | \Psi_G \rangle_{1h} \right|^2, \end{aligned} \quad (32)$$

which measures the overlap between the Bloch-wave component (cf. Eq. (7)) and the ground state ansatz (3), with $c_{\mathbf{k}\downarrow} = (1/\sqrt{N}) \sum_i e^{i\mathbf{k} \cdot \mathbf{r}_i} c_{i\downarrow}$. Note that in obtaining the second line on the rhs, $\langle c_{\mathbf{k}\sigma}^\dagger c_{\mathbf{k}\sigma} \rangle = 1/2$ (i.e., $n^e(\mathbf{k}) = 1$)

at half-filling is used due to the no double occupancy constraint.

The second quantity is the hole momentum distribution $n^h(\mathbf{k})$ defined in Eq. (12), which is the Fourier transformation of the single-hole propagator (cf. Eq. (29))

$$n^h(\mathbf{k}) = -1 + \frac{1}{N} \sum_{ij\sigma} e^{-i\mathbf{k}\cdot(\mathbf{r}_i - \mathbf{r}_j)} \left\langle c_{j\sigma} c_{i\sigma}^\dagger \right\rangle_{1h}. \quad (33)$$

Here $n^h(\mathbf{k})$ measures the momentum distribution of the hole, satisfying the sum rule

$$\sum_{\mathbf{k}} n^h(\mathbf{k}) = 1 \quad (34)$$

in the single-hole-doped case. Note that $n^e(\mathbf{k}) = 1$ or $n^h(\mathbf{k}) = 0$ at half-filling for *any* states including excited ones due to the no double occupancy constraint. So neutral spin excitations (spin currents) cannot be directly detected by such a momentum distribution. Nevertheless, beyond $Z_{\mathbf{k}}$, $n^h(\mathbf{k})$ can further show the momentum change of the bare hole due to the momentum transfer in the presence of the neutral spin current.

Figures 2(a) and (c) illustrate the hole momentum distribution $n^h(\mathbf{k})$ along the cuts of $k_y = \pm\pi/2$ at finite sizes, and the corresponding $Z_{\mathbf{k}}$'s are presented in Figs. 2(b) and (d). There are totally four peaks located at $\mathbf{K}^0 = (\pm\frac{\pi}{2}, \pm\frac{\pi}{2})$ as revealed by the calculated $Z_{\mathbf{k}}$ (cf. Fig. 1) in the ground state ansatz of Eq. (3). In particular, both $n^h(\mathbf{k})$ and $Z_{\mathbf{k}}$ in Figs. 2(a) and (b) calculated by VMC based on Eq. (3) are in excellent agreement with the DMRG results at the same sample size of 8×8 .

Furthermore, the finite size scalings of $n^h(\mathbf{k})$ and $Z_{\mathbf{k}}$ of the VMC calculation are presented in Figs. 3(a) and 3(b), where a two-component structure in the ground state $|\Psi_G\rangle$ in Eq. (3) is manifested. One is the Bloch-wave component $|\Psi_{\text{Bloch}}(\mathbf{k})\rangle$ at the momenta \mathbf{K}^0 , which gives rise to four peaks in $n^h(\mathbf{k})$ each with the weight $Z_{\mathbf{K}^0}$. However, the weight $Z_{\mathbf{K}^0}$ vanishes in a power law fashion (cf. Eq. (11)). The other is a broad distribution of the momentum with a weight $n^h(\mathbf{k}) \propto 1/N$, which makes a finite contribution to the sum rule in Eq. (34). This is consistent with the spin and charge currents presented in the ground state as shown in Figs. 5 and 6, in which the hole and the background spins share the total momentum such that the bare hole indeed behaves like an incoherent object with a broad momentum structure.

F. The $\sigma \cdot t$ -J model: Bloch-wave-like ground state

Different from the t -J model, we now consider the so-called $\sigma \cdot t$ -J model with a modified hopping term^{41,46}

$$H_{\sigma,t} = -t \sum_{\langle ij \rangle \sigma} \sigma c_{i\sigma}^\dagger c_{j\sigma} + \text{H.c.}, \quad (35)$$

where a spin-dependent sign $\sigma = \pm 1$ is attached to each hopping process of electron $c_{i\sigma}$. The superexchange term H_J remains the same as in Eq. (1). It

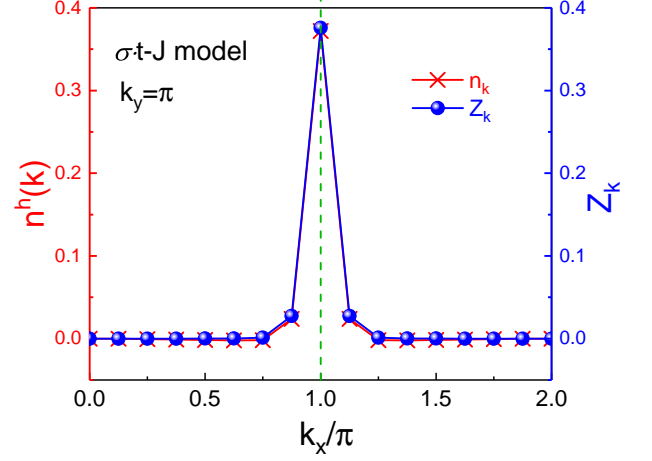


Fig. 8. (Color online) Hole momentum distribution $n^h(\mathbf{k})$ and quasiparticle weight $Z_{\mathbf{k}}$ for the $\sigma \cdot t$ -J model. Different from the t -J model in Fig. 2, $n^h(\mathbf{k})$ only has single peak located at the symmetric point $\mathbf{K}_0 = (\pi, \pi)$ with null spin currents.

can be shown that the single-hole-doped $\sigma \cdot t$ -J model has the same sign structure as the half-filled Heisenberg model, i.e., the Marshall sign structure⁴⁷. The doped hole moves in the spin background without creating additional sign mismatches. Therefore, a natural variational wave function³³ for the $\sigma \cdot t$ -J model is

$$|\Psi_G\rangle_{1h}^{\sigma \cdot t-J} = \sum_i \varphi_h(i) c_{i\downarrow} |\text{RVB}\rangle, \quad (36)$$

obtained by setting $\hat{\Pi}_i = 1$ in Eq. (16). It is nothing but the Bloch-wave state in Eq. (7) obtained in the thermodynamic limit with the translational symmetry.

By minimizing the total energy with the variational parameter φ_h in Eq. (36), the momentum distribution $n^h(\mathbf{k})$ and quasiparticle spectral weight $Z_{\mathbf{k}}$ are calculated as given in Fig. 8. Different from the t -J model, both the momentum distribution and quasiparticle weight are now sharply peaked at $\mathbf{k} = (\pi, \pi)$ without broadening. The angular momentum L_z vanishes without a novel ground state degeneracy, and there are no more spin and charge currents in the ground state. In other words, the doped hole simply reduces to a Landau type quasiparticle specified by a momentum at a symmetric point in the ground state. All are in good agreement with the ED and DMRG numerical results²⁹.

IV. DISCUSSION

To summarize, we have shown that for a single hole injected into a quantum spin background $|\text{RVB}\rangle$, its ground state is well captured by the ansatz wave function given

in Eq. (3). Specifically, such a ground state possesses a nontrivial angular momentum $L_z = \pm 1$ in 2D, which results in a novel double degeneracy at a given $S^z = \pm 1/2$. Correspondingly, hidden chiral spin currents around the hole and, *vice versa*, the chiral hole currents around the spin $S^z = \pm 1/2$ are identified by the VMC calculation. Such a single-hole state may be further decomposed into a two-component structure, with a quasiparticle component characterized by the spectral weight $Z_{\mathbf{k}}$ peaked at four momenta of $(\pm\pi/2, \pm\pi/2)$, while there emerges a broad momentum distribution due to the presence of the neutral spin current which carries away a partial momentum. These results are in excellent agreement with the finite-size DMRG calculation.

Here the wave function of a single hole in a doped Mott insulator is changed from a simple Bloch-wave to a composite one with the bare hole accompanied by a neutral spin backflow of many-body nature, i.e.,

$$\varphi_{\mathbf{h}}(i) \propto e^{i\mathbf{k}\cdot\mathbf{r}_i} \rightarrow \varphi_{\mathbf{h}}(i)e^{-i\hat{\Omega}_i}, \quad (37)$$

such that the creation operator of the quasiparticle is changed as follows

$$c_{\mathbf{k}\sigma} \rightarrow \sum_i \varphi_{\mathbf{h}}(i) \tilde{c}_{i\sigma}. \quad (38)$$

Namely, the new “twisted” hole is created by $\tilde{c}_{i\sigma} = e^{-i\hat{\Omega}_i} c_{i\sigma}$, in which the phase shift $e^{-i\hat{\Omega}_i}$ (cf. Eq. (5)) is solely responsible for the above novel ground state properties including the finite angular momentum, chiral spin/charge currents, and the double ground state degeneracy in a 2D system with the C_4 rotational symmetry. In particular, the translational symmetry is explicitly broken in the variational ground state with $\varphi_{\mathbf{h}}(i)$ no longer behaving like a Bloch wave. By contrast, $e^{-i\hat{\Omega}_i}$ disappears in the $\sigma \cdot t$ - J model (cf. the variational ground state in Eq. (7)) to restore the translational symmetry, in which the phase string effect is turned off. Clearly, $e^{-i\hat{\Omega}_i}$ is originated from the phase string effect of the t - J model.

As has been emphasized in the Introduction, the conventional spin polaron effect in the SCBA scheme leads to a coherent quasiparticle picture with a finite spectral weight $Z_{\mathbf{k}}$ and a narrow but finite bandwidth for the hole. In a Landau quasiparticle description, such a *rigid* polaron effect is expected to mainly renormalize the effective mass without leading to the novel properties discussed in the present approach and the corresponding ground state wave function is fundamentally distinct without the persistent neutral spin currents. In general, such a “longitudinal” spin polaron^{12,13,15–18} or “spin bag” effect^{34,35} may be further incorporated into the present wave function via $\hat{\Pi}_i$ in Eq. (13), which is however beyond the scope of this work.

For the present single-hole case, any thermodynamic measurement cannot be directly applied and numerical experiments have thus become very useful as employed in the present work. Nevertheless, the novel experimental implications of the present work are indeed very

important even though the ground state may be hard to be probed by the spectroscopic measurements. As pointed above, the quasiparticle picture as predicted by the SCBA has been shown to be failed as the doped hole acquires a composite structure. Consequently, it implies that in order to reconcile the well-known discrepancy between the ARPES experiment and the SCBA approach (Refs. 25–28), one should not just try to include the next-neighbor hoppings to improve the dispersion (Refs. 21–24). Rather the line-shape of broadness of the quasiparticle peak and its isotropic dispersion observed by the ARPES should be considered together as a reflection of the composite structure or fractionalization of the injected hole (Ref. 44). In particular, the waterfall phenomenon at high energy (Ref. 44) should be also understood in the framework of the fractionalization.

We may generalize the present wave function construction to more hole cases. For example, the ground state for two holes can be naturally constructed as follows

$$|\Psi_{\mathbf{G}}\rangle_{2\mathbf{h}} = \sum_{ij} g_{ij} \tilde{c}_{i\downarrow} \tilde{c}_{j\uparrow} |\text{RVB}\rangle, \quad (39)$$

which involves the pairing of two twisted holes instead of bare holes with an amplitude g_{ij} . Indeed, recent VMC calculation⁴³ for two holes in a two-leg t - J ladder has confirmed that by forming such a bound pair, two holes can significantly gain the kinetic energy by effectively cancelling out the frustration induced by the phase strings. There, the variational wave function (39) has been shown to give rise to the pair-pair correlations in excellent agreement with the DMRG result⁴⁸. For the N_h case, these twisted holes are expected to pair up in the ground state of the following form:

$$|\Psi_{\mathbf{G}}\rangle_{N_h} = \left(\sum_{ij} g_{ij} \tilde{c}_{i\downarrow} \tilde{c}_{j\uparrow} \right)^{N_h/2} |\text{RVB}\rangle, \quad (40)$$

where the no-double-occupancy constraint is automatically realized in a half-filling vacuum $|\text{RVB}\rangle$ strictly enforcing the single occupancy. According to the original RVB theory^{2,49,50}, the binding potential between holes is originated from the background RVB spin pairing, but here we emphasize that the emergent phase string effect in \tilde{c}_{\uparrow} and \tilde{c}_{\downarrow} will lead to an additional new pairing force^{43,48} which is nonlocal and dominates over the RVB pairing. Such a finite doping state has been investigated by a generalized mean-field theory^{30,51} and should be further explored by VMC in future.

V. ACKNOWLEDGEMENTS

Useful discussions with W. Zheng, Z. Zhu, J. Ho, J. Zaanen, C. Varma are acknowledged. This work is partially supported by Natural Science Foundation of China (Grant No. 11534007), MOST of China (Grant Nos. 2015CB921000 and 2017YFA0302902). Work by DNS

was supported by the Department of Energy, Office of Basic Energy Sciences, Division of Materials Sciences and

Engineering, under Contract No. DE-AC02-76SF00515 through SLAC National Accelerator Laboratory.

Appendix A: Variational ground state at half filling

At half filling, the t - J model is reduced to the spin-1/2 Heisenberg model. Anderson proposed that the ground state should be a “resonating valence bond” (RVB) state. The main assumption is that quantum fluctuations drive the two-dimensional system into a singlet state known as the spin liquid. This state can be well stimulated by Liang-Doucot-Anderson type bosonic RVB variational wave function^{33,42}:

$$|\text{RVB}\rangle = \sum_v \omega_v |v\rangle, \quad (\text{A1})$$

where

$$|v\rangle = \sum_{\{\sigma\}} \left(\prod_{(i,j) \in v} \epsilon_{\sigma_i \sigma_j} \right) c_{1\sigma_1}^\dagger \cdots c_{N\sigma_N}^\dagger |0\rangle \quad (\text{A2})$$

is a singlet pairing valence bond state with dimmer covering configuration v . Symbol $\epsilon_{\sigma_i \sigma_j}$ enables the singlet pairing between spins on site i and j . The amplitude ω_v can be factorized as $\omega_v = \prod_{(i,j) \in v} h_{ij}$ where h_{ij} is a non-negative function depending on sites i and j of different sublattices. Apparently, such a construction naturally satisfies the Marshall’s sign rule³³ due to the A - B sublattice pairings and the ϵ tensor.

Appendix B: Variational Procedure

The variational procedure involved in this work is essentially the same as presented in Ref. 33, where a single-hole-doped two-leg t - J ladder is studied by VMC method based on a ground state ansatz similar to Eq. (3). For the sake of being self-contained, in the following we outline the main procedures in the VMC calculation and one is referred to Ref. 33 for more technical details.

1. The bosonic RVB ground state $|\text{RVB}\rangle$ is optimized (Appendix A) for the superexchange term H_J at half-filling. Upon doping, the “vacuum state” $|\text{RVB}\rangle$ is unchanged as the whole change in the spin degrees of freedom as induced by the hole has been attributed to the factor Π_i in Eq. (3) generally termed the *spin polaron* effect.
2. Neglecting the whole spin polaron effect, one has a Bloch-like wave function $|\Psi_{\text{Bloch}}(\mathbf{k})\rangle_{1h}$ in Eq. (7) with momentum $\mathbf{k} = (k_x, k_y)$. The corresponding hopping term or the kinetic energy ($E_t \equiv \langle H_t \rangle$) is easily obtained by

$$E_t = 2t_{\text{Bloch}}^x \cos k_x + 2t_{\text{Bloch}}^y \cos k_y$$

with

$$\begin{aligned} t_{\text{Bloch}}^{x,y} &\equiv \frac{t}{N} \sum_{k,l} \left\langle \text{RVB} \left| c_{k\downarrow}^\dagger \left(\sum_{\langle ij \rangle \sigma} c_{i\sigma}^\dagger c_{j\sigma} + \text{h.c.} \right) c_{l\downarrow} \right| \text{RVB} \right\rangle \\ &= \frac{t}{N} \sum_{\langle ij \rangle} \frac{1}{4} (1 + 4 \langle \text{RVB} | \mathbf{S}_i \cdot \mathbf{S}_j | \text{RVB} \rangle) . \end{aligned} \quad (\text{B1})$$

The numerical simulation based on the VMC shows that $t_{\text{Bloch}}^{x,y} < 0$ which leads to the minimal energy state $|\Psi_{\text{Bloch}}(\mathbf{k})\rangle_{1h}$ at momentum $\mathbf{k} = (0, 0)$ as presented in Fig. 4(a).

3. Based on the general variational ground state ansatz in Eq. (3), the kinetic energy can be expressed by

$$E_t = - \sum_{\langle ij \rangle} \left(\tilde{H}_t \right)_{ij} \varphi_h^*(j) \varphi_h(i) + \text{h.c.} \quad (\text{B2})$$

where \tilde{H}_t is given by

$$\left(\tilde{H}_t\right)_{ij} \equiv -t \sum_{\sigma} \left\langle \text{RVB} \left| c_{j\downarrow}^{\dagger} c_{j\sigma} e^{-i(\hat{\Omega}_j - \hat{\Omega}_i)} c_{i\sigma}^{\dagger} c_{i\downarrow} \right| \text{RVB} \right\rangle, \quad (\text{B3})$$

which can be calculated³³ directly by the VMC. Similarly, we can obtain the superexchange energy $E_J \equiv \langle H_J \rangle$,

$$E_J = \sum_i (\tilde{H}_J)_i |\varphi_h(i)|^2 \quad (\text{B4})$$

with

$$(\tilde{H}_J)_i = J \sum_{\substack{\langle kl \rangle \\ k \neq i, l \neq i}} \left\langle \text{RVB} \left| e^{i\hat{\Omega}_i} \mathbf{S}_k \cdot \mathbf{S}_l e^{-i\hat{\Omega}_i} n_i^{\downarrow} \right| \text{RVB} \right\rangle. \quad (\text{B5})$$

In principle, the ground state wave function $\varphi_h(i)$ can be determined by diagonalizing a single-particle effective Hamiltonian $\hat{H}_{\text{eff}} \equiv \tilde{H}_t + \tilde{H}_J$. For a large-size square lattice, the superexchange matrix element $(\tilde{H}_J)_i$ has essentially the same value for different hole positions in the bulk due to translational symmetry. Thus, the term \tilde{H}_J plays a negligible role in determining $\varphi_h(i)$. Instead, the wave function $\varphi_h(i)$ can be optimized by directly diagonalizing \tilde{H}_t to result in E_t with a constant E_J .

-
- ¹ J. G. Bednorz and K. A. Muller, *Zeitschrift für Physik B Condensed Matter* **64**, 189 (1986).
² P. W. Anderson, *Science* **235**, 1196 (1987).
³ J. Bardeen, L. N. Cooper, and J. R. Schrieffer, *Physical Review* **108**, 1175 (1957).
⁴ P. W. Anderson, *The Theory of Superconductivity in the High-Tc Cuprate Superconductors* (Princeton University Press, 1997).
⁵ P. A. Lee, N. Nagaosa, and X.-G. Wen, *Reviews of Modern Physics* **78**, 17 (2006).
⁶ F. D. M. Haldane, in *Exactly Solvable Models of Strongly Correlated Electrons* (WORLD SCIENTIFIC, 1994) pp. 416–440.
⁷ M. Ogata and H. Shiba, in *Springer Proceedings in Physics* (Springer Berlin Heidelberg, 1990) pp. 438–443.
⁸ M. Ogata, M. Luchini, S. Sorella, and F. Assaad, *Physical Review Letters* **66**, 2388 (1991).
⁹ Y. Ren and P. W. Anderson, *Physical Review B* **48**, 16662 (1993).
¹⁰ Z.-Y. Weng, D.-N. Sheng, C. Ting, and Z. Su, *Physical Review Letters* **67**, 3318 (1991).
¹¹ Z. Zhu, Q.-R. Wang, D. Sheng, and Z.-Y. Weng, *Nuclear Physics B* **903**, 51 (2016).
¹² B. I. Shraiman and E. D. Siggia, *Physical Review Letters* **61**, 467 (1988).
¹³ B. I. Shraiman and E. D. Siggia, *Physical Review B* **42**, 2485 (1990).
¹⁴ W. F. Brinkman and T. M. Rice, *Physical Review B* **2**, 1324 (1970).
¹⁵ S. Schmitt-Rink, C. M. Varma, and A. E. Ruckenstein, *Physical Review Letters* **60**, 2793 (1988).
¹⁶ C. L. Kane, P. A. Lee, and N. Read, *Physical Review B* **39**, 6880 (1989).
¹⁷ G. Martinez and P. Horsch, *Physical Review B* **44**, 317 (1991).
¹⁸ Z. Liu and E. Manousakis, *Physical Review B* **44**, 2414 (1991).
¹⁹ E. Dagotto, *Reviews of Modern Physics* **66**, 763 (1994).
²⁰ P. W. Leung and R. J. Gooding, *Physical Review B* **52**, R15711 (1995).
²¹ P. W. Leung, B. O. Wells, and R. J. Gooding, *Physical Review B* **56**, 6320 (1997).
²² T. Tohyama, Y. Shibata, S. Maekawa, Z.-X. Shen, N. Nagaosa, and L. L. Miller, *Journal of the Physical Society of Japan* **69**, 9 (2000).
²³ W.-C. Lee, T. K. Lee, C.-M. Ho, and P. W. Leung, *Physical Review Letters* **91** (2003), 10.1103/physrevlett.91.057001.
²⁴ T. Tohyama, *Physical Review B* **70** (2004), 10.1103/physrevb.70.174517.
²⁵ B. O. Wells, Z. X. Shen, A. Matsuura, D. M. King, M. A. Kastner, M. Greven, and R. J. Birgeneau, *Physical Review Letters* **74**, 964 (1995).
²⁶ F. Ronning, C. Kim, D. L. Feng, D. S. Marshall, A. G. Loeser, L. L. Miller, J. N. Eckstein, I. Bozovic, and Z.-X. Shen, *Science* **282**, 2067 (1998).
²⁷ N. P. Armitage, D. H. Lu, C. Kim, A. Damascelli, K. M. Shen, F. Ronning, D. L. Feng, P. Bogdanov, Z.-X. Shen, Y. Onose, Y. Taguchi, Y. Tokura, P. K. Mang, N. Kaneko, and M. Greven, *Physical Review Letters* **87** (2001), 10.1103/physrevlett.87.147003.
²⁸ A. Damascelli, Z. Hussain, and Z.-X. Shen, *Reviews of Modern Physics* **75**, 473 (2003).
²⁹ W. Zheng, Z. Zhu, D. N. Sheng, and Z.-Y. Weng, *Physical Review B* **98** (2018), 10.1103/physrevb.98.165102.
³⁰ Z.-Y. Weng, *New Journal of Physics* **13**, 103039 (2011).
³¹ Z.-Y. Weng, *Frontiers of Physics* **6**, 370 (2011).

- ³² Q.-R. Wang and P. Ye, Physical Review B **90** (2014), 10.1103/physrevb.90.045106.
- ³³ Q.-R. Wang, Z. Zhu, Y. Qi, and Z.-Y. Weng, arXiv preprint arXiv:1509.01260 (2015).
- ³⁴ J. R. Schrieffer, X.-G. Wen, and S.-C. Zhang, Physical Review Letters **60**, 944 (1988); Physical Review B **39**, 11663 (1989).
- ³⁵ Z. Y. Weng, T. K. Lee, and C. S. Ting, Physical Review B **38**, 6561 (1988); Z. Y. Weng, C. S. Ting, and T. K. Lee, **41**, 1990 (1990).
- ³⁶ D. N. Sheng, Y. C. Chen, and Z. Y. Weng, Physical Review Letters **77**, 5102 (1996).
- ³⁷ Z. Y. Weng, D. N. Sheng, Y.-C. Chen, and C. S. Ting, Physical Review B **55**, 3894 (1997).
- ³⁸ K. Wu, Z. Y. Weng, and J. Zaanen, Physical Review B **77** (2008), 10.1103/physrevb.77.155102.
- ³⁹ L. Bulaevski, E. Nagaev, and D. Khomskii, Soviet Journal of Experimental and Theoretical Physics **27**, 836 (1968).
- ⁴⁰ E. Nagaev, Journal of Magnetism and Magnetic Materials **110**, 39 (1992).
- ⁴¹ Z. Zhu, H.-C. Jiang, Y. Qi, C. Tian, and Z.-Y. Weng, Scientific Reports **3** (2013), 10.1038/srep02586.
- ⁴² S. Liang, B. Doucot, and P. W. Anderson, Physical Review Letters **61**, 365 (1988).
- ⁴³ S. Chen, Z. Zhu, and Z.-Y. Weng, <http://arxiv.org/abs/1808.06173v1>.
- ⁴⁴ Z.-Y. Weng, V. Muthukumar, D.-N. Sheng, and C. Ting, Physical Review B **63**, 075102 (2001).
- ⁴⁵ T. K. Lee and C. T. Shih, Physical Review B **55**, 5983 (1997).
- ⁴⁶ Z. Zhu, H.-C. Jiang, D.-N. Sheng, and Z.-Y. Weng, Scientific Reports **4**, 5419 (2014).
- ⁴⁷ A. Auerbach, *Interacting Electrons and Quantum Magnetism* (Springer New York, 2012).
- ⁴⁸ Z. Zhu, D. Sheng, and Z.-Y. Weng, Physical Review B **97**, 115144 (2018).
- ⁴⁹ P. W. Anderson, G. Baskaran, Z. Zou, and T. Hsu, Physical Review Letters **58**, 2790 (1987).
- ⁵⁰ F. C. Zhang, C. Gros, T. M. Rice, and H. Shiba, Superconductor Science and Technology **1**, 36 (1988).
- ⁵¹ Y. Ma, P. Ye, and Z.-Y. Weng, New Journal of Physics **16**, 083039 (2014).